PONTIFICIA UNIVERSIDAD CATÓLICA DEL PERÚ

FACULTAD DE CIENCIAS E INGENIERÍA

Revisión Teórica de la técnica de Radares de Dispersión Incoherente y su conexión con las Ecuaciones Diferenciales Estocásticas

Trabajo de investigación para obtener el grado de BACHILLER EN CIENCIAS CON MENCIÓN EN FÍSICA

AUTOR

BRIAN HUMBERTO LA ROSA LA ROSA

ASESOR

MARCO ANTONIO MILLA BRAVO

Lima, diciembre, 2020

Abstract

The Incoherent Scatter Radar (ISR) technique provides an important tool for ionospheric plasma parameter estimation through the calculation of the electron density spectrum. This quantity is constrained to the ionospheric approximations considered. If these are very realistic, finding an analytical expression for the terms involve in the electron density spectrum could be impossible. In that sense, using the mathematical tool known as stochastic differential equation (SDE) is required. Because of the nature of the equation described the ionospheric particle dynamics, called Langevin equation, stochastic numerical methods have to be studied. In this work, we will present a review of ISR theory and the connection to SDE. Moreover, we list three different methods, which are used to analyze the collisional and magnetized approximation of the ionosphere.

Contents

Chapter 1

Introduction

Plasma is known as the fourth state of matter and can be described as a hot ionized gas where a combination of positive ions, electrons, and neutral species exhibit collective behaviors. The essential difference between gases and plasmas is that the latter is strongly influenced by electromagnetic interactions, despite its almost zero density charge [4]. A plasma exists because of two principal mechanisms known as ionization and recombination processes. The first one stands for removing electrons of the last electronic levels of atoms composing the plasma, because of the absorption of energy. In contrast, the recombination process stands for joining ionized atoms and electrons to form neutral species. An equilibrium of both reveals the essence for stable plasmas.

A wide range of different types of plasmas exists because of the several values their characteristic parameters can assume. The number density of charged particles, for electrons n_e, is a representative quantity for plasmas because of the information about the number of charges on a subvolume. It will lead to a differentiation between low-density and high-density plasmas. Another characteristic parameter is the Debye length λ_D, a fundamental length scale that determines the limit of action of the electric potentials on a test charge. It can be estimated from the temperature and number density of the charged particles inside the plasma [1].

As shown in figure 1, the plasma habiting the ionosphere is characterized by a low temperature and density compared to the others. This region represents the ionized portion of our atmosphere and is of importance because it participates in terrestrial and satellite communication. This work proposed a theoretical revision of the Incoherent Scatter Radar

(ISR) technique used to analyze the ionospheric plasma, including its dynamical description based on the Brownian motion process. Moreover, an introduction of the mathematical and computational tools needed to solve the dynamic equations is presented.

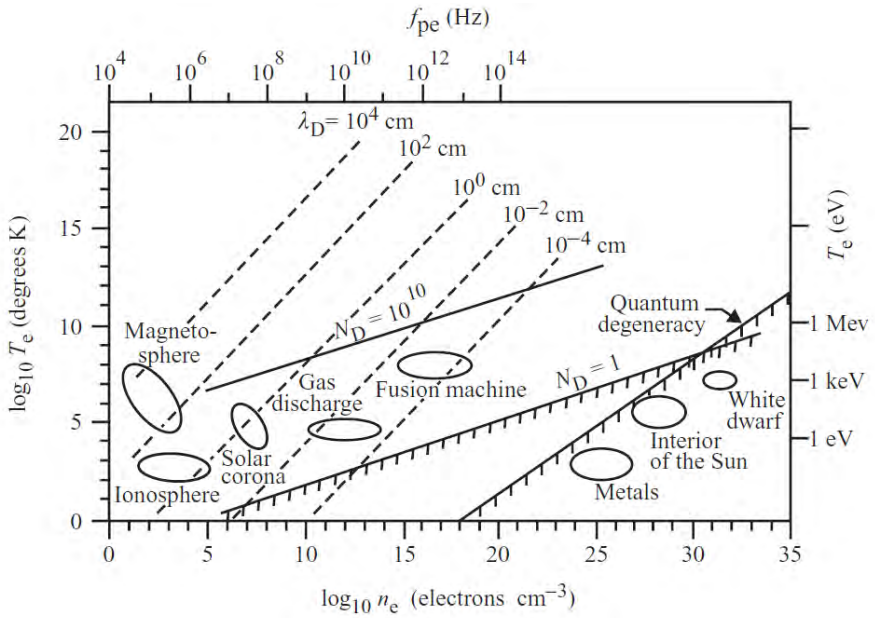

Figure 1: Temperature and density of various plasmas. [4]

This document is going to be divide as follows: In Section 2, the basis of the ISR technique is describing. Then, in Section 3, the foundation of Stochastic Differential Equations (SDE) resulting from the dynamical description of ionospheric plasma is discussing. Additionally, in Section 4, various stochastic numerical methods are used and compared taking the approximation of friction and diffusion coefficients as constants. Finally, at the end of section 4, future work is mentioned.

Chapter 2

The Incoherent Scatter Radar Theory

The Incoherent Scatter is a commonly term referring to the dispersion caused by an electromagnetic wave on a medium carried of charged particles [8]. A recognized use of this phenomenon is the incoherent scatter radar (ISR) technique. It is used to analyze the ionospheric plasmas by utilizing a set of antennas from the Earth's surface, a process known as remote sensing. In this section, a brief review of the ISR technique is presented by the study of Thomson Scattering. Then, the response of this technique is analyzed considering an ionospheric model with constant friction and diffusion coefficients.

2.1 Operating Principle

The incoherent scatter process consists of oscillating free electrons radiating as Hertzian dipoles, and results in a phenomenon known as Thomson Scattering [10]. The objective is to recover ionospheric plasma parameters by sending a well-defined electromagnetic wave from the radar. To achieve it is necessary to find the equations describing the interaction between the wave and the charges immerse in the plasma. In the next lines, we will summarize the develop made by Kudeki and Milla (2011).

The standard response of a charge (received signal by the radar), because of an incident wave, is the Hertzian dipole expression ($1 \ll \mathrm{r}$) subject to the frame of reference in figure 2:

$$\overrightarrow{E_r}(r) = E_i \frac{r_e}{r} sin(\theta) e^{-ikr} \hat{\theta} \tag{1}$$

where $E_i = E_o(\vec{r})e^{-ikr}$ describe the information of the incident wave sending by the radar, $r_e = \frac{q_e^2}{4\pi\varepsilon_0 cm^2}$ is a constant, and r is the distance between the electron and the radar. The backscatter electric field received by the antennas ($\hat{\theta} = -\hat{z}$) described in equation (1), is the response of just one electron due to the oscillation caused by the incident wave.

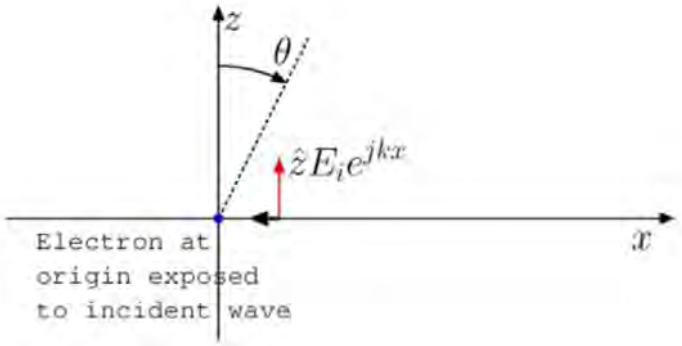

Figure 2: Hertzian dipole radiation because an incident EM wave. [10]

However, we must sum the contribution of all the electrons within a subvolume ΔV as follows (see figure 3):

$$E_s = -\frac{r_e}{r}E_i \sum_{p=1}^{N_o \Delta V} e^{i\vec{k}\cdot\vec{r_p}} \tag{2}$$

where E_s refers to the backscatter amplitude, N_0 indicates the number of electrons within de subvolume ΔV, and r_p denotes the positions of individuals electrons.

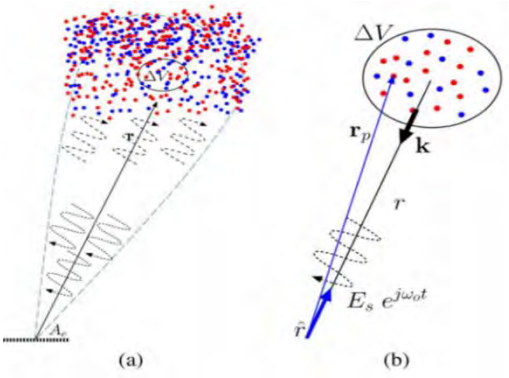

Figure 3: a) Interaction between the radar beam and the charged particles of the plasma (blue and red dots). b) Subvolume ΔV considered in the scattering process.[10]

Note that the backscatter amplitude E_s depends on the position r_p, which also depends on a retarded time $t - r/c$. As explained in reference [9] and [10], we can use the definition of the microscopic number density $n_e(\vec{r}, t)$ of the electrons within ΔV:

$$n_e(\vec{r}, t) = \sum_{p=1}^{N_o \Delta V} \delta^3 \left(\vec{r} - \overrightarrow{r_p}(t) \right) \tag{3}$$

and taking its Fourier Transform, the backscatter magnitude can be modified as

$$E_s(t) \approx -\frac{r_e}{r} E_i \sum_{p=1}^{N_o \Delta V} e^{i\vec{k} \cdot \overrightarrow{r_p}\left(t - \frac{r}{c}\right)} = -\frac{r_e}{r} E_i n_e \left(\vec{k}, t - \frac{r}{c} \right) \tag{4}$$

where the summation term represents the transformation. Thus, the space parameter $\vec{r}$ has changed to the wave vector $\vec{k}$. Nevertheless, a proper description of the backscatter electric field must be expressed in the frequency space ($t \rightarrow \omega$). A theorem known as the Wiener-Khintchine theorem establishes that the Fourier transform of an autocorrelation function (ACF) results in a power spectrum [3], thus

$$\langle |E_s(\omega)|^2 \rangle = \int e^{-i\omega\tau} \langle E_s^*(t) E_s(t + \tau) \rangle d\tau \tag{5}$$

Therefore, replacing the expression of equation (4) in (5), we obtain

$$\langle |E_s(\omega)|^2 \rangle = \frac{r_e^2}{r^2} |E_i|^2 \left\langle \left| n_e(\vec{k}, \omega) \right|^2 \right\rangle \Delta V \tag{6}$$

Note that determine the backscatter field spectrum, left side of equation (6), results in finding an expression for the electron density spectrum $\left\langle \left| n_e(\vec{k}, \omega) \right|^2 \right\rangle$. From the definition in (5), the electron density spectrum can be expanded as shown in reference [9] and [10],

$$\left\langle \left| n_e(\vec{k}, \omega) \right|^2 \right\rangle = N_0 \int d\tau e^{-i\omega\tau} \left\langle e^{-i\vec{k} \cdot \Delta\vec{r}} \right\rangle = \left\langle \left| n_{te}(\vec{k}, \omega) \right|^2 \right\rangle \tag{7}$$

where $\Delta\vec{r}$ is the electron displacement on a time τ, and the subscript n_{te} refers to the electron density spectrum taking the assumption that individual electrons follows independent random trajectories. This assumption is not valid in a real ionosphere, but this hypothetical result plays an important role in calculating the electron density spectrum in the presence of collective interactions [9]. Hence, the complete description (without the assumption) of the electron spectrum can be viewed in terms of a constant contribution (the spectrum taking the assumption) plus a perturbation as

$$n_e(\vec{r},t) = n_{te}(\vec{r},t) + \delta n_e(\vec{r},t) \tag{8}$$

Thereby, the ISR technique resumes on finding an expression for the electron density spectrum $\left\langle \left| n_e(\vec{k},\omega) \right|^2 \right\rangle$. As will be shown, this can be obtained by a linear combination of the contributions of the charged species (electrons and ions) when no collective effect is considered.

2.2 Electron Density Spectrum

According to the general framework presented previously in this section, let $n_{te}(\vec{k},\omega)$ and $n_{ti}(\vec{k},\omega)$ denote the complex amplitudes of electron and ion number density waves generated under the assumption of a plasma of non-interacting particles following independent random trajectories [9]. Conversely, $n_{e,i}(\vec{k},\omega)$ express the complete particle interaction on a real plasma (meaning that electrostatic interactions are not ignored) and can be described in terms of $n_{te,i}(\vec{k},\omega)$. First, consider the next Ampere's Law:

$$\nabla \times \vec{\mathrm{H}} = \vec{\mathrm{J}} + \varepsilon_0 \frac{\partial \vec{E}}{\partial t} \tag{9}$$

where the total electron current density $\vec{J}$ along the direction of the wave vector $\vec{k}$ results in the superposition of two parts: the macroscopic currents $\sigma_e E$ and $\sigma_i E$ (where σ_s express the

conductivity of the specie s), and a contribution equals to $\frac{\omega}{k}e(n_{te}-n_{ti})$, because of an imbalance in the space charged density between the independent random variables $n_{te,i}(\vec{k},\omega)$ [10]. The equation of Ampere's law results:

$$0=(\sigma_i+\sigma_e)E+\frac{\omega}{k}e(n_{ti}-n_{te})+i\omega\varepsilon_0 E \tag{10}$$

The equation above is equivalent to an electrical circuit applied to the plasma species. As we need an expression for the electron density amplitude $n_e(\vec{k},\omega)$, the equivalent circuit for electrons must be solved $-\omega k^{-1}en_e=E\sigma_e-\omega k^{-1}en_{te}$. Isolating the electric field E and then replacing in equation (10), we obtain

$$n_e(\vec{k},\omega)=\frac{(i\omega\varepsilon_0+\sigma_i)n_{te}(\vec{k},\omega)+\sigma_e n_{ti}(\vec{k},\omega)}{i\omega\varepsilon_0+\sigma_e+\sigma_i} \tag{11}$$

Note that $n_{te,i}(\vec{k},\omega)$ are independent random variables as we are considering the assumption of independent random trajectories. Then, we can find the electron density spectrum by squaring and averaging:

$$\left\langle\left|n_e(\vec{k},\omega)\right|^2\right\rangle=\frac{|i\omega\varepsilon_0+\sigma_i|\left\langle\left|n_{te}(\vec{k},\omega)\right|^2\right\rangle}{|i\omega\varepsilon_0+\sigma_e+\sigma_i|^2}+\frac{|\sigma_e|^2\left\langle\left|n_{ti}(\vec{k},\omega)\right|^2\right\rangle}{|i\omega\varepsilon_0+\sigma_e+\sigma_i|^2} \tag{12}$$

This spectrum expression is a general result valid not only with a singular type of ion, but we can also include more in the current density treatment ($\vec{J}$) and use it in the Ampere's law [10]. To have a complete description of the equation (12), conductivities must be known. In general, these are complex quantities and requires the use of two extra relationships.

Note that have a complete representation of a complex number means having both real and imaginary coefficients. Kramers-Kronig relations provides the connection between these two parts, where the imaginary part $Im[\sigma_{e,i}(\vec{k},\omega)]$ can be identified as a Hilbert transform of the

real part $Re[\sigma_{e,i}(\vec{k},\omega)]$. Moreover, according to the fluctuation-dissipation theorem, a relation between $Re[\sigma_{e,i}(\vec{k},\omega)]$ and the spectrum $\langle|n_{te,i}(\vec{k},\omega)|^2\rangle$ is provided. In summary, determines a complete representation of conductivities $\sigma_{e,i}(\vec{k},\omega)$, results in finding the spectrum $\langle|n_{te,i}(\vec{k},\omega)|^2\rangle$. Therefore, it turns out that the density spectrum on a real plasma $\langle|n_{e,i}(\vec{k},\omega)|^2\rangle$ is completely solved by utilizing $\langle|n_{te,i}(\vec{k},\omega)|^2\rangle$, which denotes the electron and ion density spectrum under the assumption of particles following independent random trajectories. For a more detail explanation of both, Kramers-Kronig relations and fluctuation dissipation theorem, see references [9] and [10].

Finally, determine the electron density spectrum $\langle|n_{te,i}(\vec{k},\omega)|^2\rangle$ described in equation (7) simplifies in finding the characteristic function:

$$\left\langle e^{i\vec{k}\cdot\Delta\vec{r}}\right\rangle = \int f(\Delta r)\, e^{i\vec{k}\cdot\Delta\vec{r}}\, d(\Delta r) \tag{13}$$

which also turns out to be determined if the displacement probability distribution function $f(\Delta r)$ is known. However, specifying the pdf $f(\Delta r)$ means solving the dynamic equations of plasma species for a large number of different trajectories (statistical approach) or solving the Boltzmann equation for the pdf $f(\Delta r)$ (plasma kinetic approach). Note that the dynamic equations are constrained to the level of ionospheric plasma realism considered.

An appropriate description of the ionospheric plasma complexity must regard the contribution of the charged particles interaction known as Coulomb collisions. It can be modeled in Newton's second law as the influence of two forces: friction and diffusion forces. However, different from other scenarios, these forces are stochastic contributions, leading to a reconsider the dynamic interaction as a Langevin equation.

Furthermore, different as its name suggests, Coulomb collisions are not collisions in the complete sense. It describes the electromagnetic force interaction between charged particles at a microscopic level. In other words, particles are constantly deflected by this force when they get nearer. It is the effect we want to recover modeling the contributions of friction and diffusion forces.

To exemplify, using the statistical approach, we will not use the more complex model when friction and diffusion coefficients are variable with velocity as shown in reference [11]. Instead, a collisional approximation (friction and diffusion coefficients as constants) and magnetized ionosphere is considered in the treatment of this work.

2.3 Brownian Motion in a Magnetized Ionosphere

The incoherent scatter radar approximation allows us to simplify the estimation of plasma parameters calculating the probability distribution function of the charged particles displacements $f(\Delta r)$. In general, this cannot result in an easy task. As mention before, it can be achieved by solving analytically the full Boltzmann Kinetic equation [4]. Nevertheless, despite some available solutions for simplified versions, determining the pdf results in a difficult task, and sometimes, there is no solution. Alternatively, simulating a large set of particle trajectories permits to recover some statistical quantities. However, the stochastic natural behavior of equations describing particle velocities adds a different kind of complication explained later in this section. Using the latter approximation, statistical approach, the pdf $f(\Delta r)$ will be calculated considering a first collisional approximation on magnetized ionosphere.

First, the dynamics described by the motion of charged particles in a plasma, constraint to a constant random contribution of the Brownian motion process, can be described with a Langevin equation as:

$$\frac{\mathrm{d}\vec{v}(t)}{\mathrm{d}t} = A(\vec{v},t) + \tilde{C}(\vec{v},t)W(t) \tag{14}$$

where A is a vector and $\tilde{C}$ a matrix whose arguments are $\vec{v}$ and t. Also, $\mathrm{W}(t)$ is a random vector with gaussian independent components [6]. Note that the second term in the right side of equation (14) is a fluctuating force which stands for Brownian Motion defined as $W(t_2) - W(t_1) = \sqrt{t_2 - t_1}N(0,1)$, where $N(0,1)$ denote a random normal distribution with mean $\mu = 0$ and unit variance [5]. $W(t)$ is a vector that contributes equal and independently in each velocity direction.

A special case of Markovian process (or continuous memoryless stochastic process) occurs when $A(\vec{v},t) = -\beta\vec{v}$ and $\tilde{C} = D^{1/2}I_3$, used in the approximation of constant friction and diffusion coefficients [Kudeki milla], where D is the diffusion coefficient and I_3 stands for a unitary 3×3 matrix. Furthermore, the fluctuating force $M(t) = \tilde{C}W(t)$ must satisfy the property of Gaussian white noise correlation function [6].

$$\langle M_i(t)M_j(t+\tau)\rangle = D\delta_{ij}\delta(\tau) \tag{15}$$

where the suffix (i,j) denotes the component direction.

Let us rewrite the equation in terms of the new variables, adding the magnetic force because of the $\vec{B}$ field contribution

$$\frac{\mathrm{d}\vec{v}}{\mathrm{d}t} = \frac{q}{m}\vec{v}\times\vec{B} - \beta\vec{v} + D^{1/2}W(t) \tag{16}$$

To determine the pdf $f(\Delta r)$, we will assume a Gaussian distributed displacement and calculate the corresponding variance, which can be calculated analytically from the solution of the Langevin equation (16). Before that, we can make an appropriate change of coordinates where the last component is parallel to the magnetic field $\vec{B}$. This will be useful in calculating the variance. Therefore, consider an orthogonal rotation matrix

$$R(t) = \begin{pmatrix} cos\ \omega_B t & sin\ \omega_B t & 0 \\ -sin\ \omega_B t & cos\ \omega_B t & 0 \\ 0 & 0 & 1 \end{pmatrix} \tag{17}$$

where $\omega_B = q\left|\vec{B}\right|/m$. Then, the analytic solution of equation (16) considering the rotation can be expressed as indicated in Jimenez (2006)

$$\vec{v}'(t) = e^{-\beta t} R(t)\overrightarrow{v_0}' + R(t)\int_0^t e^{-\beta(t-s)}\, R^T(s) M(s) ds \tag{18}$$

when the prime symbol denotes the new coordinate system.

Before to calculate the variance of the displacement, we need to calculate the correlation function for the velocity $\vec{v}'(t)$ at two different times. To do that, we assume an initial Maxwell distribution function for velocity. As shown in [6], the correlation function for velocity read as

$$\begin{aligned} \left\langle \overrightarrow{v_i}'(t_1)\vec{v}_j{}'(t_2)\right\rangle = {} & \frac{k_B T}{m} e^{-\beta(t_1+t_2)} R_{ik}(t_1) R_{jk}(t_2) \\ & + \frac{D}{2\beta} R_{ik}(t_1) R_{jk}(t_2)\left[e^{-\beta(t_1-t_2)} - e^{-\beta(t_1+t_2)}\right] \end{aligned} \tag{19}$$

where k_B is the Boltzmann constant and T is the plasma species temperature. D can be calculated from the condition when $t_1 = t_2 = t$, and times goes to infinity. In that case, Brownian particle must be in thermal equilibrium as follows from the equipartition theory of classical statistical thermodynamics

$$\frac{1}{2} m\left\langle v'^2(t)\right\rangle = \frac{3k_B T}{m} e^{-2\beta t} + \frac{3Dm}{4\beta}\left[1 - e^{-2\beta t}\right] = \frac{3k_B T}{2} \tag{20}$$

from which is obvious that $D = 2k_B T\beta/m$. [6]

Using the last results, we can perform the variances for the vector position defined commonly as $d\vec{r}'(t)/dt = \vec{v}'(t)$. Then, if at $t = 0$ the particle is in $\vec{r}'(0)$, the mean square displacement can be defined as

$$\left\langle \left(\vec{r}'(t) - \vec{r}'(0)\right)^2 \right\rangle = \sum_{i=1}^{3} \int_0^t \int_0^t \left\langle \overrightarrow{v_i}'(t_1)\overrightarrow{v_i}'(t_2) \right\rangle dt_1 dt_2 \tag{21}$$

Note that the equations (19) and (20) can be employed to solve equation (21). If we rename the directions as $\vec{r}'(t) = \left(x'(t), y'(t), z'(t)\right)$, we obtain first for the z' direction (which is parallel to $\vec{B}$)

$$\left\langle \left(\vec{z}'(t) - \vec{z}'(0)\right)^2 \right\rangle = \frac{k_B T}{m} \left[\int_0^t \int_0^t e^{|t_1 - t_2|} dt_1 dt_2 \right] \tag{22}$$

$$\langle (\Delta z')^2 \rangle = \frac{2v_{th}^2}{\beta^2} \left(\beta t - 1 + e^{-\beta t}\right) \tag{23}$$

where $v_{th} = (k_B T/m)^{1/2}$ is the thermal velocity. Then, for the x' and y'(both perpendicular to $\vec{B}$), we obtain

$$\langle (\Delta x')^2 \rangle = \langle (\Delta y')^2 \rangle = \frac{k_B T}{m} \left[\int_0^t \int_0^t cos\omega(t_1 - t_2)\, e^{|t_1 - t_2|} dt_1 dt_2 \right] \tag{24}$$

$$\langle (\Delta x')^2 \rangle = \langle (\Delta y')^2 \rangle = \frac{2v_{th}^2}{\beta^2 + \omega^2} \left(cos(2\gamma) + \beta t - e^{-\beta t} cos(\omega t - 2\gamma) \right) \tag{25}$$

where $\gamma = tan^{-1}\beta/\omega$ [10].

Having the variances which contains the information about this spectra model (considering an ambient $\vec{B}$ field and constant friction and diffusion coefficients), we can find the probability density function $f(\Delta r)$. As explained before, this is used to obtain the electron density spectrum $\left\langle \left| n_{e,i}(\vec{k}, \omega) \right|^2 \right\rangle$, and consequently, the ionospheric plasma parameters.

The recovery of analytic expressions for the variances could be impossible if we increment the realism of the ionospheric plasma model. For instance, if we consider charged particles undergoing Coulomb collisions with friction and diffusion coefficients dependents of speed

$|\vec{v}|$, there is no analytic solution available [10]. Despite this new complexity, we can still calculate the pdf $f(\Delta r)$ by solving numerically the corresponding Langevin equation. To calculate the variances, and so the pdf $f(\Delta r)$, we must solve for a large set of different particle trajectories. Then, using a Monte Carlo approach, the statistics can be obtained.

Nevertheless, solving an SDE is not trivial. As the Langevin equation corresponds to that kind of equations, we must focus on the complications this approximation implies. In the next section, an introduction to SDEs and three different numerical algorithms to solve them are presented.

Chapter 3

Stochastic Differential Equations

The deterministic calculus, developed mainly by Newton and Leibnitz, allowed us to build a variety of dynamical systems from many areas of scientific research. However, stochastic effects must be considered if more realistic models are required. Stochastic calculus, known as Ito calculus, describes the dynamic systems when randomness is essential to model a phenomenon [12]. As mention before, ionospheric particle dynamics are described by the Langevin equation (14), and, because of its stochastic nature, it is relevant to understand the behavior of this type of equations. In this section, an introduction to SDE theory is provided. Then, some stochastic numerical methods are presented and studied.

3.1 A first approach to SDE theory

Stochastic equations are used in many research areas, however, all of them maintain almost the same structure. Let us consider the following one-dimensional SDE of the form

$$dX_t = a(X_t)dt + b(X_t)dW_t \tag{26}$$

defined on the interval $I[0,T]$, with the initial condition $X(t=0) = X_0$. This equation consists of two parts: a slowly varying component corresponding to the drift coefficient a, and a rapid random fluctuation associated to the diffusion coefficient b [12]. Note that the second differential in the right side of the equation is respect to a Wiener process, also known as standard Brownian Motion.

The main difference between the deterministic classical calculus and the stochastic calculus is that the path of a Wiener process is not differentiable [5]. From the stochastic chain rule, is more obvious what is the meaning of this

$$df(X_t) = \left(f'(X_t)a(X_t) + \frac{1}{2} f''(X_t)b^2(X_t) \right) dt + f'(X_t)b(X_t)dW_t \qquad (27)$$

where an extra term proportional to $f''(X_t)$ in the drift function, provides the essential difference between deterministic and SDE numerical methods [12].

3.2 Stochastic Numerical Methods

As mention previously, the dynamic system equation of a phenomenon undergoing randomness contributions, must be solved for stochastic numerical algorithms. The complexity of these can vary because of the precision required to solve the equation. Similar to the deterministic case, more terms involving the numerical method results in a more accurate estimation. Next, we list three methods:

1) **Euler-Maruyama method**

   The Euler-Maruyama method, applied on the general form of the SDE in (26), takes the form

   $$X_{n+1} = X_n + a(X_n)\Delta t + b(X_n)\Delta W; \quad n = 1,2,..L \qquad (28)$$

   where Δt is the time-step used for the numerical simulation along the interval $I[0,T]$, and $L = T/\Delta t$ is number of steps. Also, defined as a standard Brownian motion, $\Delta W = W(t_{n+1}) - W(t_n)$ is a normally distributed random variable with mean zero and variance $\Delta t = t_{n+1} - t_n$, or equivalently, $\Delta W = \sqrt{\Delta t}\, N(0,1)$, where $N(0,1)$ denotes a normally distribution random variable with mean zero and unit variance [5].

This algorithm is the simplest of the stochastic methods. It is the first approximation in the stochastic Taylor expansion, and no second-order terms are involved [7]. Note that if $b \equiv 0$ and X_0 is constant, we return to the deterministic case known as Euler's Method. Despite this simple approximation, it could be used in a wide range of problems, as in the asset price model in financial mathematics, where good approximations are obtained [5]. Also, as described in reference [11], this method is used to calculate the ionospheric particle statistics even when variable friction and diffusion coefficients are considered. However, while more complex is the phenomenon, a higher computational performance is needed. For this reason, higher-order and accurate computational methods have been developed.

2) Richardson Extrapolated method

A wide range of stochastic numeric methods, which produce more accurate results, has been developed in the last decades. In 1990, Talay and Tubaro proposed a numerical algorithm known as the Richardson extrapolated method. It belongs to a family of algorithms known as extrapolated methods, which take advantage of less precise methods to obtain more accuracy. In particular, the Richardson extrapolated method makes use of the Euler-Maruyama approach described before [12]. It takes the following form

$$Y_{g,2}^{\Delta}(T) = 2E\left[g\left(X^{\Delta}(T)\right)\right] - E\left[g\left(X^{2\Delta}(T)\right)\right] \tag{29}$$

where $X^{\delta}(T)$ denotes the value at time T of the Euler-Maruyama approach with time-step equals to δ, and $Y_{g,2}^{\Delta}(T)$ denotes the more accurate result. The idea is that taking the difference of the expectation terms $E\left[g\left(X^{\delta}(T)\right)\right]$, the leading error coefficients

cancels out [12]. Hence, we obtain a better approximation against Euler-Maruyama method.

3) Stochastic Runge-Kutta (Platen 1999)

A more accurate numerical algorithm was the stochastic method proposed by Platen in 1999 [7]. It is from the family of the stochastic Runge-Kutta approximations shown in reference [2]. However, this version provides a free-derivative approximation that allow us to reduce the calculation when the coefficients of equation (25) are more complex. The method reads as follows

$$X_{n+1} = X_n + \left(a(\widehat{X_n}) + a(X_n)\right)\frac{\Delta t}{2} + \left(b(X_n^+) + b(X_n^-)\right)\frac{\Delta \widehat{W}_n}{4} + \left(b(X_n^+) - b(X_n^-)\right)\left((\Delta \widehat{W}_n)^2 - \Delta t\right)\frac{1}{4\sqrt{\Delta t}} \tag{30}$$

with

$$\widehat{X_n} = X_n + a(X_n)\Delta t + b(X_n)\Delta \widehat{W_n} \tag{31}$$

and

$$X_n^{\pm} = X_n + a(X_n)\Delta t \pm b(X_n)\sqrt{\Delta t} \tag{32}$$

where $\Delta \widehat{W_n}$ is a three-point distributed random variable with $P\left(\Delta \widehat{W_n} = \pm\sqrt{3\Delta t}\right) = 1/6$ and $P(\Delta \widehat{W_n} = 0) = 2/3$. Different to the previous methods, is clearly that more precision requires adding various terms in the discretization.

All the above methods can be expanded into higher dimensions if it is required to the dynamic system of interest. It is important to note that to recover statistical quantities, you must use these methods to solve a large set of simulations. Hence, you must find the best stochastic method which give an adequate balance between the precision required, and the computational cost of each of these methods need. For example, a high-order algorithm from the family of the

stochastic Runge-Kutta methods can be used to have higher precision, but you must deal with all terms involving the discretization and the computational effort it introduces. Conversely, you should use a simple approximation as Euler-Maruyama, but you must deal with the low accuracy of the simulation. Moreover, as we required statistical quantities, we must multiply these complications by the number of simulations needed.

3.3 Weak and Strong convergence

Previously in this section, three algorithms had been presented. Each method can be used to solve the general form of the SDE shown in equation (26). These methods differ in the precision that each of them can achieve at solving the equation, however, we still have not provided a rigorous form to analyze it. Therefore, an introduction to the order of convergence is presented.

First, a SDE numerical method is said to have a strong order of convergence equal to γ if exists a constant C such

$$E|X_n - X(t_n)| \leq C\Delta t^{\gamma} \tag{33}$$

where the left part of the inequality denotes the expected value of the error between the analytic value X_n and the simulation $X(t_n)$, at a time $t = n\,\Delta t$ [5]. Strong convergence suggests a strictly restrictive relation. It affirms that the mean of the absolute error of a large set of simulations, is enclose by the right side of (32). In other words, the simulation is required to be constantly close to the exact solution.

On the other hand, a method is said to have weak order of convergence of order γ if exists a constant C such that

$$\left|E[g(X_n)] - E\left[g\left(X(t_n)\right)\right]\right| < C\Delta t^{\gamma} \tag{34}$$

In contrast to the strong convergence, the left part of the inequality denotes that the error of the expected value of a dependent function $E[g(X_n)]$ compared to the simulated expected value $E\left[g\left(X(t_n)\right)\right]$, are delimited. In this case, it is not important the exact solution of the variable X_n, but to keep the tendency of functions evaluated in this variable.

Note that all stochastic methods have both, strong and weak order of convergence, which are not necessarily equal. There are methods which has a higher strong order of convergence, but low weak order of convergence, and the reverse. As we are interested on statistical quantities, which are functions that depends on the dynamic variables, methods with higher weak order of convergence are required.

Chapter 4

Numerical Analysis of SDEs

4.1 Weak convergence analysis on a one-dimensional SDE

As mention before, numerical SDE methods can be classified by their strong or weak order of convergence. We already listed three different algorithms, but no test has been done yet. Therefore, we will examine the weak order of convergence by using a one-dimensional SDE.

First, to analyze the weak order of convergence γ of each method, we need to stablish the following relation derived from equation (34)

$$log\ e_{\Delta t}^{weak} = log\ C + \gamma\ log\Delta t \tag{35}$$

where the inequality has been converted into an equation. Also, a ten based logarithm has been taken, and $e_{\Delta t}^{weak}$ denotes the difference between the expected values $\left|E[g(X_n)] - E\left[g\left(X(t_n)\right)\right]\right|$ calculated with a time-step Δt. The idea is solving for a least square method, considering $log\ \Delta t$ as an x-axis, $log\ e_{\Delta t}^{weak}$ as a y-axis and γ as the slop of the curve. Hence, we obtain a straight-line approximation where each point denotes the error between the exact value and the simulation calculated with a time-step Δt.

To exemplify this, consider the following SDE of the form

$$dX_t = \left(\frac{1}{2}X_t + \sqrt{X_t^2 + 1}\right)dt + \sqrt{X_t^2 + 1}dW_t\,; \quad \mathrm{X}(0) = 0 \tag{36}$$

with analytic solution $X_t = sinh(t) + W_t$.

To analyze the weak order of convergence γ, consider a time interval $I[0,2]$ and a function $g(x) = p\big(archsin(x)\big)$, where $p(z) = z^3 - 6z^2 + 8z$ is a polynomial. Also, the expectation of the solution can be calculated as shown in [2]

$$E\big(g(X_t)\big) = t^3 - 3t^2 + 2t \tag{37}$$

Finally, the solution of $E\big(g(X_t)\big)$ is approximated with step sizes $2^{-1}, 2^{-2}, 2^{-3}, 2^{-4}$, and a number $N = 10^6$ of different simulations were performed to calculate the numerical expectation.

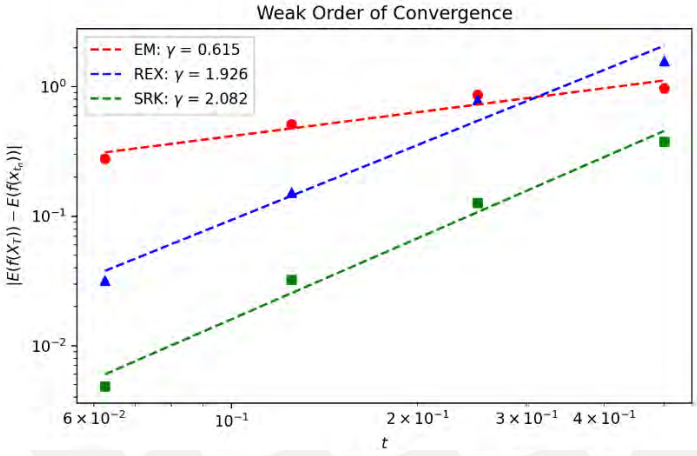

Figure 4: Weak order of convergence is shown using the SDE (35). The analysis for Euler Maruyama, Richardson extrapolated method and stochastic Runge-Kutta (proposed by Platen) are in colors red, blue, and green, respectively. The four dots in each line are for each time-step value.

These methods are particularly useful when statistical quantities are required. From figure 4, we can observe two features: the first one is concern to the method itself. The error associated to each one is reduced when time step is decreased. Also, the way that these errors decrease with the time step is as straight line with slope equals to γ. From the literature, it is known that the order of convergence is $\gamma = 1$ for Euler-Maruyama, and $\gamma = 2$ for the others two methods. The second feature is that in order of accuracy, Euler-Maruyama is the less precise, and, despite Richardson extrapolation and stochastic Runge-Kutta have the same order of convergence, the

latter is more accurate. This is consequent with the fact that if the method has a bigger discretization, the simulation is more precise.

4.2 Monte Carlo simulation of the Woodman's Model

The Woodman's (1967) model considers a collisional and magnetized ionosphere but taking the friction and diffusion coefficients as constants. The expression of the dynamics was described in equation (16), but we can be more explicit and separate it in three dimensions

$$d\begin{pmatrix} v'_x \\ v'_y \\ v'_z \end{pmatrix} = \begin{pmatrix} v'_y\omega_B - \beta v'_x \\ -v'_x\omega_B - \beta v'_y \\ -\beta v'_z \end{pmatrix} dt + \begin{pmatrix} D_\perp^{1/2} & 0 & 0 \\ 0 & D_\perp^{1/2} & 0 \\ 0 & 0 & D_\parallel^{1/2} \end{pmatrix} d\begin{pmatrix} W_1 \\ W_2 \\ W_3 \end{pmatrix} \tag{38}$$

remember that v'_z is parallel to the $\vec{B}$ field and the prime symbol is due to the change of coordinates of the rotation matrix in (17). Also, $\omega_B = qB/m$ is the gyrofrequency and the diffusion matrix is diagonal with $D_\perp^{1/2} = D_\parallel^{1/2} = (2k_B T\beta/\mathrm{m})^{1/2}$ because of the approximation taken.

As we are interested in computing the statistical quantities (variances) numerically, previously calculated analytically in (23) and (25), we will use the three methods mentioned above to solve the velocity equation (38). To achieve this, we must follow the next steps: first, to compute the particle velocity described in equation (16) we can use each of the methods listed above. However, the multidimensional extension to each algorithm must be considered, such we are working with a velocity vector. These extensions are found in reference [7]. Then, the velocity vector must be integrated over time to obtain the particle displacement $\Delta\vec{r}$. Finally, the variances $\langle(\Delta x')^2\rangle$, $\langle(\Delta y')^2\rangle$ and $\langle(\Delta z')^2\rangle$ are calculated by averaging a large set of particles.

Note that in figure 5, the simulation has been done with the next settings: first, the friction coefficient is equal to $\beta = 5.88\,Hz$, and the diffusion coefficient follows the constrain $D = 2k_B T\beta/m$. Additionally, $T = 1000\,K$ and the mass m is for oxygen ions O^+. Then, the initial velocity condition is assumed to be a random normal distributed $N(0, v_{th})$. Last, a time step $\Delta t = 10^{-4}\,s$ and a number $N = 10\,000$ of different particle trajectories were simulated within the time interval $I[0,0.5]$ in seconds.

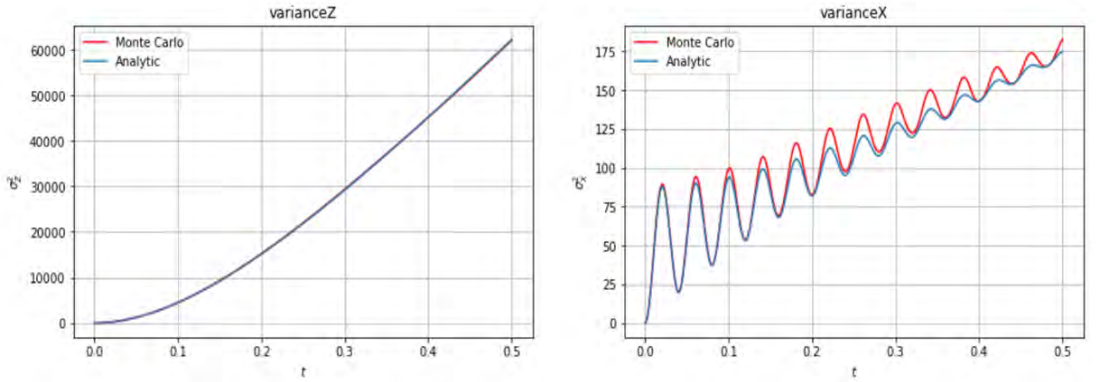

(a)

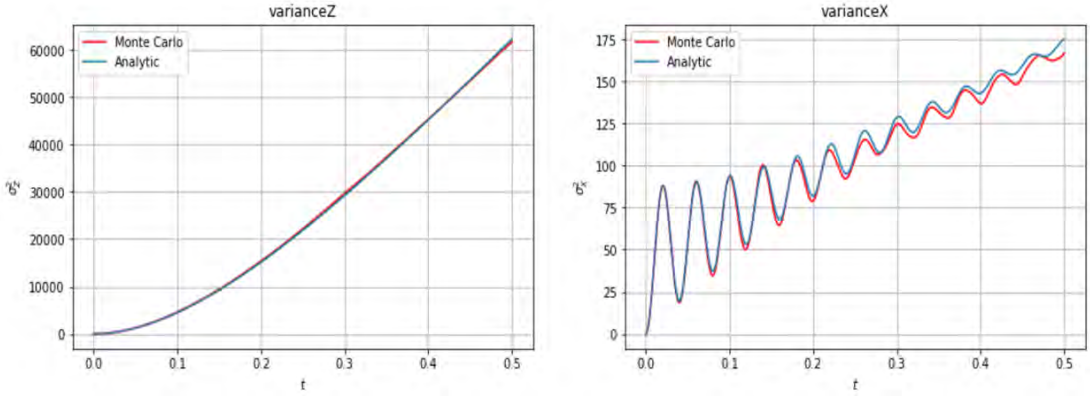

(b)

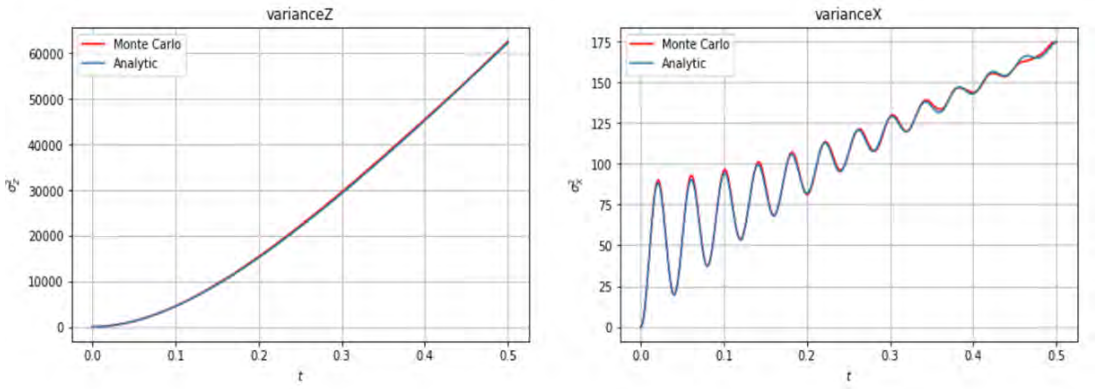

(c)

Figure 5: Parallel z' (left plot) and perpendicular x', y' (right plot) variances has been simulated for each SDE method listed in this work. In blue are plotted the analytic expressions (equations (23) and (25)), and in red are plotted the simulations (a) Euler-Maruyama (b) Richardson Extrapolation (c) Stochastic second order Runge-Kutta

From the graphics, a clear increment of accuracy is observed for higher-order algorithms as the shapes of both curves are nearer. This suggests that without the necessity of increasing the number of trajectories for the Monte Carlo, a reduction in the absolute error is obtained. However, we must pay the computational effort for the extra terms used in the higher-order algorithms.

4.3 Future Work

This work intends to present a theoretical review of ISR technique and SDEs. Moreover, the importance to study SDE theory when no analytic solution is available has been discussing. In addition, we are interested to show the availability of other higher-order algorithms and their potential to perform better stochastic analysis, as many times required in ionosphere research. Richardson extrapolated method and stochastic weak second order Runge-Kutta are potential alternatives against the Euler-Maruyama scheme. The most important extension to this work is to complete the analysis for the methods listed here by convergence and linear

stability tests. Then, produce an SDE analysis but in the complete Milla and Kudeki (2011) description, where the friction and diffusion coefficients are variable and take the form of Spitzer coefficients [11].

Bibliography

[1] Chen, Francis F. (2016). *Introduction to Plasma Physics and Controlled Fusion.* New York, USA. Editorial: Springer.

[2] Debrabant, K. \& Robler, A. (2008). Classification of stochastic Runge–Kutta methods for the weak approximation of stochastic differential equations. Mathematics and computers in simulation, vol 77, pp 408-420. doi: 10.1016/j.matcom.2007.04.016

[3] Dechant, A. & Lutz, Eric (2015). Wiener-Khinchin theorem for nonstationary scale-invariant processes. *Physical Review Letters*, vol 115, pp 080603. doi: https://doi.org/10.1103/PhysRevLett.115.080603

[4] Gournet, D. & Bhattacharjee, A. (2005). *Introduction to Plasma Physics with Space and Laboratory Applications*. New York, USA. Editorial: Cambridge University Press.

[5] Higham, Desmond J. (2001). An algorithmic introduction to numerical simulation of stochastic differential equations. *Society for Industrial and Applied Mathematics*, vol 43(3), pp 525–546. doi: 10.1137/S0036144500378302

[6] Jimenez-Aquino \& Romero-Bastida (2006). Brownian motion of charged particle in a magnetic field. Mexican Journal of Physics, 52(2), 182-187. Available in: http://www.scielo.org.mx/scielo

[7] Kloeden, Peter E. & Platen, Eckhard (1999). *Numerical Solution of Stochastic Differential Equations*. Berlin, Germany. Editorial: Springer.

[8] Kloeden, Peter & Platen, Eckhard (1994). *Numerical solution of SDE through computer experiments.* Berlin, Germany. Editorial: Springer.

[9] Kudeki, Erhan (2006). Lectures Notes on Applications of Radiowave Propagation. *Department of Electrical and Computer Engineering, University of Illinois Urbana - Champaign.*

[10] Kudeki, E. & Milla, M.A. (2011). Incoherent scatter spectral theories-Part I: A general result for small magnetic aspect angles. *IEEE Transactions on Geoscience and Remote Sensing*, vol 49, pp 315-328. doi: 10.1109/TGRS.2010.2057252

[11] Milla, M.A. & Kudeki, E. (2011). Incoherent scatter spectral theories-Part II: A general result for small magnetic aspect angles. *IEEE Transactions on Geoscience and Remote Sensing*, vol 49, pp 329 - 345. doi: 10.1109/TGRS.2010.2057253

[12] Platen, Eckhard (1999). An introduction to numerical methods for stochastic differential equations. *Acta Numerica*, vol 8, pp 197-246. doi: 10.1017/S0962492900002920

[13] Prolss, G. (2003). *Physics of the Earth's space environment.* Berlin, Germany. Editorial: Springer

[14] Rosin, M.S. et al (2014). Multilevel Monte Carlo simulation of Coulomb collisions. *Journal of Computational Physics,* vol 274, pp 140-157. doi: https://doi.org/10.1016/j.jcp.2014.05.030

[15] Saito, Yoshiro & Mitsui, Takemoto (1996). Stability analysis of numerical schemes for stochastic differential equations. *SIAM Journal of Numerical Analysis*, vol 33(6), pp 2254-2267. Doi: https://doi.org/10.1137/S0036142992228409

[16] Spitzer, L. (1962). *Physics of fully ionized gases*. New York, USA. Editorial: Wiley-Interscience.

[17] Sulzer, Michael P. & Gonzáles, Sixto (1999). The effect of electron Coulomb collisions on the incoherent scatter spectrum in the F region at Jicamarca. *Journal of Geophysical Research*, vol 104, pp 22 535-22 551. doi: 10.1029/1999JA900288

[18] Uhlenbeck, G. & Onstein, L. (1930). On the theory of Brownian motion. *Physical Review,* vol 36(5), pp 823-841. doi: https://doi.org/10.1103/PhysRev.36.823